

# Hydrogen trapping in metallic glasses investigated by positron annihilation and differential scanning calorimetry

R. PAREJA\*, J. M. RIVEIRO\*, A. JEREZ†

\* *Departamento de Física de la Materia Condensada, Facultad de Ciencias Físicas and*

† *Departamento de Química Inorgánica, Facultad de Ciencias Químicas, Universidad Complutense, 28040 Madrid, Spain*

Positron annihilation experiments have been performed on the metallic glasses  $\text{Co}_{58}\text{Ni}_{10}\text{Fe}_5\text{B}_{16}\text{Si}_{11}$ ,  $\text{Fe}_{78}\text{B}_{13}\text{Si}_9$  and  $\text{Fe}_{81}\text{B}_{13.5}\text{Si}_{3.5}\text{C}_2$  produced by melt-spinning. For the metallic glass  $\text{Co}_{58}\text{Ni}_{10}\text{Fe}_5\text{B}_{16}\text{Si}_{11}$  it has been found that the positron lifetime spectrum is either single-component or resolvable in two exponential terms, depending on the production parameters of the ribbons. The commercial metallic glass  $\text{Fe}_{78}\text{B}_{13}\text{Si}_9$  (2605S2) shows a two-component spectrum while the alloy  $\text{Fe}_{81}\text{B}_{13.5}\text{Si}_{3.5}\text{C}_2$  (2605SC) exhibits a single-component spectrum. After hydrogen charging no significant changes are observed in the positron lifetime of those metallic glasses which exhibit a single-component spectrum. For ribbons showing a two-term spectrum, the intensity of the long-lived component  $I_2$  decreases with the cumulative charging time. This decrease is interpreted in terms of hydrogen trapping in the structural defects responsible for the long-lived component. Differential scanning calorimetry of ribbons of  $\text{Co}_{58}\text{Ni}_{10}\text{Fe}_5\text{B}_{16}\text{Si}_{11}$  suggest that hydrogen in extended structural defects should induce some local structural change.

## 1. Introduction

In recent years the study of hydrogen behaviour in metallic glasses has been a subject of increasing interest for practical applications of these materials as well as for insights into the relationship between structural defects and physical properties. Hydrogen in metallic glasses has been investigated using techniques such as internal friction [1, 2], nuclear magnetic resonance [3], magnetic after-effect [2], neutron scattering [4], micro-calorimetry and thermal analysis [5-8] and electrochemical methods [9, 10] among others. However, at this present time there exist few reports on annihilation experiments in hydrogenated metallic glasses.

Early positron annihilation experiments carried out by Mô and Moser [2] in the amorphous alloy  $\text{Fe}_{40}\text{Ni}_{40}\text{P}_{14}\text{B}_6$  hydrogen-charged electrolytically suggested that positrons might not be sensitive to hydrogen in metallic glasses, in spite of the fact that internal friction and magnetic after-effect measurements revealed the presence of hydrogen in the structure. According to previous suggestions by Berry and Pritchett [1], the results were interpreted in terms of hydrogen localization in empty small interstitial positions of the structure which surrounded extended structural defects. To explain why positrons are not sensitive to hydrogen, Mô and Moser [2] have argued that it is because hydrogen is actually located away from the centre of the extended defects responsible for positron trapping.

On the other hand, it is well known that defects such as vacancies, dislocations and impurities are effective traps for hydrogen in crystalline metals, so that the

defect concentration and type in the host lattice can be quite an important determining factor of hydrogen behaviour in crystalline metals [11]. Hence positron annihilation has been applied as a probe for studying hydrogen trapping by defects in crystalline metals [12-15]. The hydrogen molecule dissociates upon absorption by metals, and in the case of transition metals the proton diffusion will characterize the hydrogen behaviour in the sample. Since protons and positrons are very similar particles it seems that both particles should be trapped in the same defects. In fact, the experimental evidence shows that protons and positrons in crystalline metals become trapped in the same defects. In these materials, the presence of hydrogen in vacancy-like defects effectively reduces the positron lifetime in these defects [14, 15] although the positron binding energy in a vacancy containing hydrogen may be similar to that in an empty vacancy according to calculations [16].

Consequently, we think that positron annihilation should be a convenient probe for acquiring further knowledge of the relationship between hydrogen behaviour and structural defects in metallic glasses. The aim of the present work has been to investigate this point by means of positron annihilation experiments in several metallic glasses charged electrolytically with hydrogen. In addition, differential scanning calorimetry (DSC) experiments were carried out for some of the metallic glasses herein studied in order to get additional information about hydrogen absorption in these alloys.

## 2. Experimental details

In this work the following amorphous alloys, made by melt-spinning on a rotating wheel, have been used:  $\text{Co}_{58}\text{Ni}_{10}\text{Fe}_5\text{B}_{16}\text{Si}_{11}$ ,  $\text{Fe}_{78}\text{B}_{13}\text{Si}_9$  and  $\text{Fe}_{81}\text{B}_{13.5}\text{Si}_{3.5}\text{C}_2$ .

Two different ribbons of the home-made alloy  $\text{Co}_{58}\text{Ni}_{10}\text{Fe}_5\text{B}_{16}\text{Si}_{11}$ , having different production parameters, were studied. Samples of this alloy, 25 mm long and labelled No. 1, were cut from a ribbon 3.5 mm wide having the following production parameters:

Wheel rotation velocity:  $\Omega = 6 \times 10^3$  r.p.m.

Melt temperature:  $T_m = 1573$  K

Ejection pressure:  $p = 1.3$  atm

Incident angle:  $\alpha = 90^\circ$

Calculated contacting time  
with the wheel:  $t = 25$  msec

Thickness:  $z = 24$   $\mu\text{m}$

As-cast ribbon coercivity:  $H_c = 12$  mOe

Another set of samples of the same alloy, also 25 mm long and labelled No. 2, were prepared from a ribbon also 3.5 mm wide obtained under the following conditions:  $\Omega = 6 \times 10^3$  r.p.m.,  $T_m = 1273$  K,  $p = 1.3$  atm,  $\alpha = 30^\circ$ ,  $t = 0.8$  msec,  $z = 33$   $\mu\text{m}$  and  $H_c = 5.4$  mOe ( $0.43$  A  $\text{m}^{-1}$ ). The amorphous structure of both ribbons was checked by X-ray diffraction using  $\text{FeK}\alpha$  radiation. A complete absence of peaks corresponding to crystalline structure was observed.

The other two metallic glasses,  $\text{Fe}_{78}\text{B}_{13}\text{Si}_9$  (2605S2) and  $\text{Fe}_{81}\text{B}_{13.5}\text{Si}_{3.5}\text{C}_2$  (2605SC), were obtained from Allied Corporation, Parsippany, New Jersey. Samples 10 mm wide and 25 mm long were prepared from ribbons of these two alloys which were 25 mm wide and approximately 32  $\mu\text{m}$  thick.

After performing positron annihilation measurements in the as-cast samples, they were hydrogen-charged in an electrolytic cell using the samples as cathode and a platinum foil as anode. The electrolytic bath consisted of a 0.1 N  $\text{H}_2\text{SO}_4$  solution containing 10 p.p.m. of  $\text{NaAsO}_3$  as a hydrogen recombination inhibitor. The charge current was approximately 600 A  $\text{m}^{-2}$  and the bath temperature was kept at 292 K during charging. Each set of samples was hydrogen-charged successively for several periods of time; in the case of the samples of  $\text{Fe}_{78}\text{B}_{13}\text{Si}_9$ ,  $\text{Fe}_{81}\text{B}_{13.5}\text{Si}_{3.5}\text{C}_2$  and  $\text{Co}_{58}\text{Ni}_{10}\text{Fe}_5\text{B}_{16}\text{Si}_{11}$  (No. 1a) until they lost their integrity when handled. The hydrogen content in the samples was not determined in these experiments but it is assumed that it increases with the cumulative charging time. After each electrolytic charge, the samples were stored at room temperature for two days before positron annihilation measurements in order to allow hydrogen to diffuse through the samples. Moreover, similar experiments were made on another sample set of the alloy  $\text{Co}_{58}\text{Ni}_{10}\text{Fe}_5\text{B}_{16}\text{Si}_{11}$  (No. 1) labelled No. 1b, which was previously annealed at 623 K for 3 h in purified argon.

Positron lifetime measurements were performed at room temperature using a conventional fast-fast spectrometer having a time resolution of 310 psec at full width at half maximum (FWHM) for the  $^{60}\text{Co}$

prompt peak. A  $^{22}\text{Na}$  source of about  $7 \times 10^5$  Bq on a 0.7 mg  $\text{cm}^{-2}$  nickel foil was sandwiched between five or six layers of samples in order to be sure that practically all positrons were annihilated inside the samples. The spectra were collected up to get a total number of counts of about  $6 \times 10^5$ .

For the as-cast and hydrogen-charged alloys  $\text{Co}_{58}\text{Ni}_{10}\text{Fe}_5\text{B}_{16}\text{Si}_{11}$ , DSC experiments were carried out in a Mettler TA3000 thermoanalyser equipped with a DSC 30 cell. The enthalpy released during crystallization was calculated by integration of the crystallization peaks, taking into account a suitable correction for the baseline.

## 3. Results and discussion

### 3.1. Positron annihilation

After subtracting two appropriate source corrections the lifetime spectra were analysed using the program POSITRONFIT EXTENDED [17]. The results are summarized in Table I.

It was found that the samples of  $\text{Co}_{58}\text{Ni}_{10}\text{Fe}_5\text{B}_{16}\text{Si}_{11}$  exhibit different lifetime spectra depending on the production parameters of the ribbons. In the case of the Sample Nos 1a and 1b, the spectra can be analysed in terms of two components but this could not be done for Samples No. 2. For the samples of  $\text{Fe}_{78}\text{B}_{13}\text{Si}_9$ , a second component is also observed in the lifetime spectrum. Nevertheless the samples of  $\text{Fe}_{75}\text{B}_{13.5}\text{Si}_{3.5}\text{C}_2$ , as-cast or hydrogen-charged, always exhibit a single-component spectrum like the samples of  $\text{Co}_{58}\text{Ni}_{10}\text{Fe}_5\text{B}_{16}\text{Si}_{11}$  (No. 2).

Previously, it has been reported that positron trapping in metallic glasses depends on their production parameters and furthermore, that the long-lived component observed in certain metallic glasses scaled with the quenching rate [18–21]. This long-lived component has been attributed to positron trapping in extended structural defects whose extension and number should depend on the production conditions of the alloy. Since the ribbon of  $\text{Co}_{58}\text{Ni}_{10}\text{Fe}_5\text{B}_{16}\text{Si}_{11}$  (No. 1) should undergo a higher quenching rate than the ribbon of No. 2, we associate the second lifetime component observed in Sample Nos 1a and 1b to positron trapping in these kind of defects which would be absent or almost absent in Samples No. 2.

In order to minimize the dispersion of  $I_2$  values obtained from the unconstrained analyses, the spectra were analysed keeping the long lifetime value  $\tau_2$  constrained to an average value. It should be noted that an unconstrained analysis does not resolve two components in the spectrum of the samples of  $\text{Co}_{58}\text{Ni}_{10}\text{Fe}_5\text{B}_{16}\text{Si}_{11}$  (No. 1a) and  $\text{Fe}_{78}\text{B}_{13}\text{Si}_9$  after hydrogen charging for 45 and 16 min, respectively. The unconstrained analyses show that after successive hydrogen charging, the intensity of the long-lived component  $I_2$  decreases without significant change in the long lifetime value  $\tau_2$ . It can be observed that this effect is common to those samples showing a two-component lifetime spectrum. However, in spite of this decrease the mean lifetime  $\bar{\tau} = (1 - I_2)\tau_1 + I_2\tau_2$  does not seem to change significantly after hydrogen charging. These results for the samples of  $\text{Co}_{58}\text{Ni}_{10}\text{Fe}_5\text{B}_{16}\text{Si}_{11}$  (Nos 1a and 1b) and  $\text{Fe}_{78}\text{B}_{13}\text{Si}_9$

TABLE I Annihilation parameters along with the time of hydrogen charging. Here  $\tau_1 = \lambda_1^{-1}$  and  $\tau_2 = \lambda_2^{-1}$ , where  $\lambda_1$  and  $\lambda_2$  are the decay rates of the first and second spectral component.  $I_2$  is the intensity of the second component,  $\bar{\tau} = (1 - I_2)\tau_1 + I_2\tau_2$  is the mean positron lifetime,  $\tau_s^{-1} = \lambda_s$  the decay rate of the single-component spectrum, and  $\lambda_0$  the annihilation rate given by Equation 1

Sample	Treatment	Cumulative charging time (min)	Single-component analysis: $\tau_s$ ( $\times 10^{-12}$ sec)	Two-component analysis				$\lambda_0$ ( $\times 10^9$ sec $^{-1}$ )
				$\tau_1$ ( $\times 10^{-12}$ sec)	$\tau_2$ ( $\times 10^{-12}$ sec)	$I_2$ (%)	$\bar{\tau}$ ( $\times 10^{-12}$ sec)	
Co <sub>38</sub> Ni <sub>10</sub> Fe <sub>5</sub> B <sub>16</sub> Si <sub>11</sub> (No. 1a)	As-cast	—	—	103 ± 6	247 ± 6	37 ± 3	156	7.61
	Hydrogen-charged	15	—	110 ± 3*	250	35.0 ± 0.6	159	7.31
		30	—	131 ± 5	262 ± 24	17 ± 4	153	6.93
		45	—	125 ± 2*	250	22.3 ± 0.7	153	7.11
Co <sub>38</sub> Ni <sub>10</sub> Fe <sub>5</sub> B <sub>16</sub> Si <sub>11</sub> (No. 1b)	Annealed at 623 K for 3 h	—	168 ± 2	142 ± 2	255 ± 23	17 ± 6	161	6.51
		—	—	144 ± 2*	250	15.9 ± 1.2	161	6.45
		—	—	155 ± 2*	250	9.4 ± 1.7	164	6.22
		—	—	104 ± 7	230 ± 7	39 ± 4	153	7.56
Co <sub>38</sub> Ni <sub>10</sub> Fe <sub>5</sub> B <sub>16</sub> Si <sub>11</sub> (No. 2)	Hydrogen-charged	15	—	118 ± 3*	250	28.9 ± 0.8	156	7.18
		90	—	109 ± 6	245 ± 7	37 ± 3	159	7.29
		—	—	120 ± 2*	250	29.0 ± 0.8	158	7.08
		—	—	145 ± 6	258 ± 25	12 ± 3	159	6.53
Fe <sub>78</sub> B <sub>13</sub> Si <sub>9</sub>	Hydrogen-charged	10	156 ± 2	115 ± 19	196 ± 14	53 ± 8	158	6.79
		20	158 ± 1	122 ± 5*	205	43.0 ± 2.1	158	6.77
		40	153 ± 2	121 ± 14	211 ± 17	40 ± 9	157	6.85
		60	155 ± 1	120 ± 5*	205	41.1 ± 1.9	155	6.91
Fe <sub>81</sub> B <sub>13.5</sub> Si <sub>3.5</sub> C <sub>2</sub>	Hydrogen-charged	2	—	128 ± 16	206 ± 20	41 ± 9	160	6.60
		8	—	127 ± 4*	205	40.4 ± 1.6	159	6.66
		16	162 ± 2	—	—	—	—	—
		—	—	152 ± 5*	205	13 ± 6	161	6.36

\* Annihilation parameters obtained constraining the  $\tau_2$  value to a fixed value.

can be explained if hydrogen is trapped in the structural defects responsible for the long-lived component. Hydrogen in these defects would reduce the lifetime  $\tau_2$  because the local atom density increases. However, it is expected that hydrogen in these defects does not involve an appreciable diminution of the positron trapping rate according to experimental evidence [12–15] and calculations of the positron annihilation characteristics in vacancies containing hydrogen [16, 22]. This reduction could be high enough so that positron annihilation in extended defects containing hydrogen contributes to the short-lived component. So, after hydrogen charging the short-lived component resulting from a two-component analysis would represent a merged component. If the current two-state model were assumed for positrons in these alloys, the annihilation rate of the first state,  $\lambda_0$ , could be obtained using the known equation [23]

$$\lambda_0 = \lambda_1 - (\lambda_1 - \lambda_2)I_2 \quad (1)$$

where  $\lambda_1 = \tau_1^{-1}$  and  $\lambda_2 = \tau_2^{-1}$  are the decay rates of the respective exponential terms; the  $\lambda_0$  values are shown in Table I. It is observed that  $\lambda_0$  is not constant, decreasing simultaneously with  $I_2$  which means that  $\lambda_0$  will not actually be the annihilation rate of a positron state. This supports the above suggestion of treating the short-lived component as a merged component.

The annealed samples of  $\text{Co}_{58}\text{Ni}_{10}\text{Fe}_5\text{B}_{16}\text{Si}_{11}$  (No. 1b) exhibit a  $\tau_2$  value of  $230 \pm 7$  psec which is quite similar to the value of  $247 \pm 6$  psec obtained for the as-cast alloy and not significantly different from the values obtained after hydrogen charging. In these samples, the lower decreasing rate of  $I_2$  with charging time might suggest a lesser efficiency for hydrogen charging induced by annealing. Changes in the hydrogen solubility, when metallic glasses are annealed, have been attributed to structural changes induced by annealing [9]. Nevertheless, it is rather difficult to discern if this is due either to an effective structural change induced by annealing in the extended traps, or to unavoidable fluctuations of the current during charging. It might also be due to passivation of the sample surfaces; however, it should be noted that in order to try removing the poisoned layer from the surface, the samples were dipped in an acid solution and carefully cleaned up after each hydrogen charging and prior to the positron annihilation measurements.

Although significant changes do not take place in the lifetime spectrum of the alloys  $\text{Co}_{58}\text{Ni}_{10}\text{B}_{16}\text{Si}_{11}$  (No. 2) and  $\text{Fe}_{81}\text{B}_{13.5}\text{Si}_{3.5}\text{C}_2$  upon hydrogen charging, their embrittlement is evidence that hydrogen is effectively incorporated into the structure of these alloys. If according to Berry and Pritchett [1] it is assumed that in these two alloys the interstitial empty holes of the amorphous structure are the sites where hydrogen is localized, the occupancy of the equilibrium sites for hydrogen could be given after Kirchheim's model [9, 10] as

$$O(G) = n(G) / \left[ 1 + \exp\left(\frac{G - \mu}{RT}\right) \right] \quad (2)$$

where  $G$  is the free enthalpy of hydrogen in the site,  $\mu$  the chemical potential of hydrogen and  $n(G)$  the

density of sites for hydrogen given by a Gaussian function. It is easy to see that at room temperature there has to be a high number of these interstitial sites free of hydrogen. Since these interstitial holes should also be positron traps, as currently accepted, the number of these sites free of hydrogen after charging may be high enough that all positrons are trapped even after a long period of charging. This would account for the insensitivity of positron lifetime to hydrogen charging in the case of the alloys  $\text{Co}_{58}\text{Ni}_{10}\text{Fe}_5\text{B}_{16}\text{Si}_{11}$  (No. 2) and  $\text{Fe}_{81}\text{B}_{13.5}\text{Si}_{3.5}$ .

### 3.2. DSC measurements

In order to obtain additional evidence supporting the above account for hydrogen trapping in the alloys  $\text{Co}_{58}\text{Ni}_{10}\text{Fe}_5\text{B}_{16}\text{Si}_{11}$  (Nos 1 and 2), DSC experiments were carried out with as-cast and hydrogen-charged samples. Fig. 1 shows the DSC traces obtained for the as-cast and hydrogen-charged alloys. The DSC traces from the as-cast samples are identical for both alloys. However after hydrogen charging for 30 min, a noticeably endothermic process takes place for Alloy No. 1 over a wide temperature range above 633 K which is absent from Alloy No. 2. Heating-cooling cycles performed over the range 0 to 765 K did not meaningfully change the trace shape of this endothermic process. This fact rules out that the endothermic process can be attributed to hydrogen desorption, suggesting that it could be due to some structural changes in certain regions where hydrogen is trapped. The absence of this endothermic process for the alloy

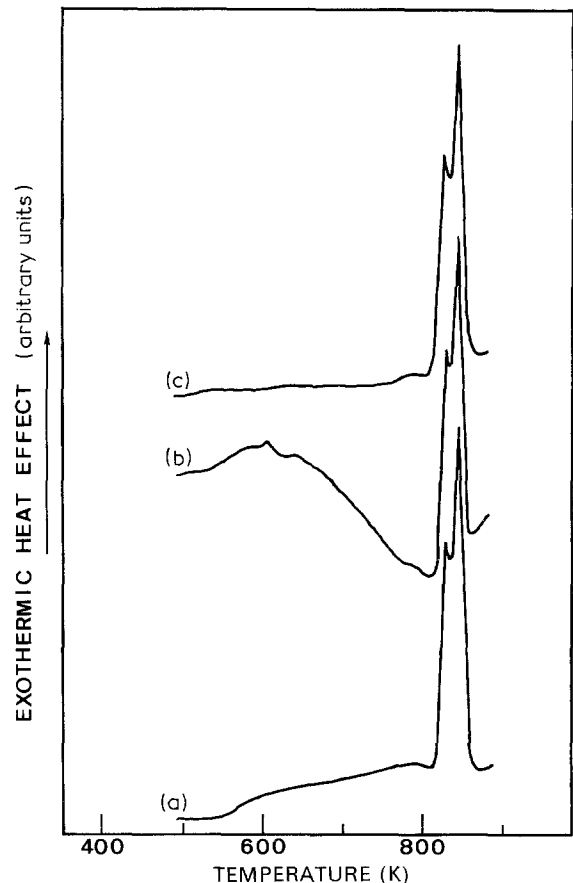


Figure 1 DSC traces obtained at  $10 \text{ K min}^{-1}$ . Curves (a) and (b) from the as-cast and 30 min hydrogen-charged alloy  $\text{Co}_{58}\text{Ni}_{10}\text{Fe}_5\text{B}_{16}\text{Si}_{11}$  (No. 1), respectively, and Curve (c) from the 90 min hydrogen-charged alloy  $\text{Co}_{58}\text{Ni}_{10}\text{Fe}_5\text{B}_{16}\text{Si}_{11}$  (No. 2). The exothermic peaks are due to crystallization.

$\text{Co}_{58}\text{Ni}_{10}\text{Fe}_5\text{B}_{16}\text{Si}_{11}$  (No. 2) after hydrogen charging for more than 1 h reveals that certain kinds of hydrogen trap, which were present in Alloy No. 1, either do not exist in Alloy No. 2 or are almost absent. The onset of crystallization for a heating rate of  $10\text{ K min}^{-1}$  appears at 803 K for both alloys, independent of whether the samples are hydrogen-charged or not. However, for the alloy  $\text{Co}_{58}\text{Ni}_{10}\text{Fe}_5\text{B}_{16}\text{Si}_{11}$  (No. 1) the enthalpy released during crystallization is significantly reduced when the sample is hydrogen-charged;  $99.4\text{ J g}^{-1}$  for the as-cast alloy against  $90.6\text{ J g}^{-1}$  for the alloy hydrogen-charged for 30 min. On the other hand, no meaningful changes in the released enthalpy are observed for the alloy  $\text{Co}_{58}\text{Ni}_{10}\text{Fe}_5\text{B}_{16}\text{Si}_{11}$  (No. 2) after hydrogen-charging for more than 1 h. Structural changes induced by hydrogen in the alloy  $\text{Co}_{58}\text{Ni}_{10}\text{Fe}_5\text{B}_{16}\text{Si}_{11}$  might account for the discrepancies in the released enthalpy.

#### 4. Conclusions

In the case of those metallic glasses exhibiting a positron lifetime spectrum resolvable into two exponential terms, hydrogen trapping is observed in the structural defects responsible for the second spectral component. For the metallic glasses exhibiting a single-component spectrum, positron lifetime is not sensitive to hydrogen charging in spite of the evidence for hydrogen absorption by the samples.

Positron and hydrogen trapping in metallic glasses obtained by the melt-spinning method depend on the production parameters of the ribbon. The results suggest the existence of two kinds of trap for positrons and hydrogen. Those which are deeper are likely to be associated with extended structural defects which should be present in the more rapidly quenched alloys. The other traps would be the interstitial holes of the amorphous structure.

The positron annihilation results and the DSC experiments in the alloys  $\text{Co}_{58}\text{Ni}_{10}\text{Fe}_5\text{B}_{16}\text{Si}_{11}$  suggest that hydrogen in extended structural defects should induce some local structural change.

#### References

1. B. S. BERRY and W. C. PRITCHET, *Scripta Metall.* **15** (1981) 637.

2. C. M. MÔ and P. MOSER, *Phys. Status Solidi (a)* **78** (1983) 201.
3. R. C. BOWMAN and A. J. MAELAND, *Phys. Rev. B* **24** (1981) 2328.
4. J. J. RUSH, J. M. ROWE and A. J. MAELAND, *J. Phys. F* **10** (1980) L 283.
5. R. C. BOWMAN, R. J. FURLAN, J. S. CANTRELL and A. J. MAELAND, *J. Appl. Phys.* **56** (1984) 3362.
6. R. A. DUNLAP and K. DINI, *J. Phys. F* **14** (1984) 2797.
7. K. DINI and R. A. DUNLAP, *ibid.* **15** (1985) 273.
8. A. J. MAELAND, L. E. TANNER and G. G. LIBOWITZ, *J. Less-Common Metals* **74** (1980) 279.
9. R. KIRCHHEIM, F. SOMMER and G. SCHLÜCKEBIER, *Acta Metall.* **30** (1982) 1059.
10. R. KIRCHHEIM, *ibid.* **30** (1982) 1069.
11. C. A. WERT, in "Hydrogen in Metals", Vol. II, edited by G. Alefeld and J. Volkl (Springer, Berlin, 1978) p. 305.
12. B. LENGELER, S. MANTL and W. TRIFTSHÄUSER, *J. Phys. F* **8** (1978) 1691.
13. G. M. HOOD and R. J. SCHULTZ, *Scripta Metall.* **16** (1982) 1359.
14. C. S. SUNDAR, A. BHARATHI and K. P. GOPINATHAN, *Phil. Mag. A* **50** (1984) 635.
15. P. HAUTOJÄRVI, H. HUOMO, M. PUSKA and A. VEHANEN, *Phys. Rev. B* **32** (1985) 4326.
16. P. JENA and M. J. PONNAMBALAM, *ibid.* **24** (1981) 2884.
17. P. KIRKEGAARD and M. ELDRUP, *Comput. Phys. Commun.* **7** (1974) 401.
18. Z. KAJCSOS, L. MARCZIS, A. LOVAS, E. KISDIKOSZO, D. KISS, C. SZELES and G. BRAUER, *Nucl. Instr. Meth.* **199** (1982) 327.
19. Z. KAJCSOS, L. MARCZIS, L. GRANASY, C. SZELES, D. KISS, A. LOVAS and G. BRAUER, in "Positron Annihilation", edited by P. G. Coleman, S. C. Sharma and L. M. Diana (North-Holland, 1982) p. 601.
20. Z. KAJCSOS, L. GRANASY, T. KEMENY, L. F. KISS, E. KISDI-KOSZO, G. KONCZOS, A. LOVAS, L. MARCZIS, C. SZELES and G. BRAUER, in "Positron Annihilation", edited by P. C. Jain, R. M. Singru and K. P. Gopinathan (World Scientific, Singapore, 1985) p. 921.
21. Z. KAJCSOS, R. PAULIN, F. BOILEAU, A. LOVAS, L. MARCZIS and A. ASHRY, in "Positron Annihilation", edited by P. C. Jain, R. M. Singru and K. P. Gopinathan (World Scientific, Singapore, 1985) p. 935.
22. K. IYAKUTTI, J. L. CALAIS and A. H. TANG KAI, *J. Phys. F* **13** (1983) 1.
23. R. W. SIEGEL, *Ann. Rev. Mater. Sci.* **10** (1980) 393.

Received 2 March

and accepted 29 April 1987